CRITICAL CONDUCTION MODE BUCK-BUCK/BOOST CONVERTER WITH HIGH EFFICIENCY

A. Hakeem Memon
IICT, Mehran UET, Jamshoro.
E-mail: hakeem.memon@faculty.muet.edu.pk

Mansoor A. Memon
IICT, Mehran UET, Jamshoro.
E-mail: mansoorjali74@gmail.com

Zubair A. Memon
IICT, Mehran UET, Jamshoro.
E-mail: zubair.memon@faculty.muet.edu.pk

Ashfaque A. Hashmani
IICT, Mehran UET, Jamshoro.
E-mail: ashfaque.hashmani@faculty.muet.edu.pk

Recepción: 31/07/2019 **Aceptación:** 23/09/2019 **Publicación:** 06/11/2019

Citación sugerida:
Memon, A.H., Memon, M.A., Memon, Z.A. y Hashmani, A.A. (2019). Critical Conduction Mode Buck-Buck/Boost Converter with High Efficiency. *3C Tecnología. Glosas de innovación aplicadas a la pyme. Edición Especial, Noviembre 2019*, 201-219. doi: http://dx.doi.org/10.17993/3ctecno.2019.specialissue3.201-219

Suggested citation:
Memon, A.H., Memon, M.A., Memon, Z.A. & Hashmani, A.A. (2019). Critical Conduction Mode Buck-Buck/Boost Converter with High Efficiency. *3C Tecnología. Glosas de innovación aplicadas a la pyme. Speciaal Issue, November 2019*, 201-219. doi: http://dx.doi.org/10.17993/3ctecno.2019.specialissue3.201-219

ABSTRACT

The buck converter is commonly utilized in various low power applications because of maintaining high efficiency at universal input voltage and many other advantages. On the other hand, when the on-time is constant, the conduction and switching losses are more because the rms and peak value of the inductor current is more. So, the efficiency is low. For improving efficiency, a variable on-time control (VOTC) strategy has been proposed for buck-buck/boost topology with simple structure, minimum losses and less component cost. For verifying the validity of proposed technique, the simulation results are carried out by using saber simulator.

KEYWORDS

Variable on-time control (VOTC), Constant on-time control (COTC), Critical conduction mode (CRM), Buck/boost converter, Buck converter.

DOI: http://dx.doi.org/10.17993/3ctecno.2019.specialissue3.201-219

1. INTRODUCTION

Power electronic technology is used in various types of modern equipment's which has made our life easier, simpler and luxurious. However, this technology is based on semiconductor devices, due to which the shape of average input current is distorted. The distorted current has various drawbacks such as voltage distortion, increased power loss and noise etc. So the industries have built various standards such as IEC61000-3-2 limit and IEEE 519 (International Electrotechnical Commission, 2014; Langella, Testa, & Alii, 2014). Therefore, various types of power factor correction (PFC) converters are put forward in the literature to improve the shape of distorted current (García, Cobos, Prieto, Alou, & Uceda, 2003; Singh, Singh, Chandra, & Al-Haddad, 2011) and the buck converter is one of them. Its advantages include protection against short circuit, high efficiency at universal input voltage, low output voltage, and less voltage stress on the switch. However, its input power factor (PF) is low due to dead zone in the average input current. Integrating buck converter with buck/boost converters can solve the dead zone problem and enhance its PF. On the other hand, when the on-time is constant, the conduction and switching losses are more because the rms and peak value of the inductor current is more. So, the efficiency is low. Thus, it is necessary for the integrated buck-buck/boost converter to propose the technique which can attain high efficiency with simple structure and minimum losses.

For modifying the performance of traditional buck converter, various researches have proposed various control strategies and topologies.

Spiazzi and Buso (2000) have proposed a new solution for eliminating the dead zone in the buck converter. It has proposed flyback converter to work with buck converter during dead zone period. Alonso, Dalla Costa, and Ordiz (2008) have implemented integrated buck-flyback converter (IBFC) for low cost, high PF and fast output voltage regulations. Dalla Costa, Alonso, Miranda, García, and Lamar (2008) have presented IBFC for single-stage electronic ballast with high PF. Gacio, Alonso, Calleja, Garcia, and Rico-Secades (2011) have presented offline IBFC for high brightness light emitting diode (HB-LED) to cover the application of LED in street light. Xie, Zhao,

Lu, and Liu (2013) have put forward a new topology which combines buck and flyback converter to eliminate the dead zone. Zhang, Zhao, Zhao, and Wu (2017) have proposed a topology which combines buck converter with flyback converter. Yao *et al.* (2017) have proposed an injecting third harmonic method to realize high PF. Memon, Yao, Chen, Guo, and Hu (2017) have put forward a control scheme is put forward to improve input PF. Memon *et al.*, (2019) have introduced flyback converter to work with buck converter for boundary conduction mode (BCM) buck converter to enhance PF. Memon *et al.*, (2019) have introduced buck/boost converter to work with buck converter for BCM buck converter to enhance PF. Memon *et al.*, (2019) have proposed control technique to improve input PF of integrated buck-flyback converter.

In this paper, a variable on-time control (VOTC) strategy is introduced for critical conduction mode (CRM) buck-buck/boost converter to attain high efficiency with simple structure, minimum losses and minimum component cost. It requires one bridge rectifier (BR) and for passing the low frequency current to reduce losses, EMI filter is located after BR.

The analysis of the operating principle of buck converter is discussed with traditional control (COTC) scheme in Section 2. The VOTC is put forward in Section 3 to attain efficiency. In Section 4, power loss analysis is given. Section 5 deals with simulation results and the conclusion are given in Section 6.

2. OPERATION ANALYSIS OF CRM BUCK-BUCK/BOOST PFC CONVERTER

Figure 1 illustrates the schematic diagram of buck-buck/boost converter. The major components in the power circuit are: Bridge rectifier (*BR*); an inductor (*L*); a buck switch (Q_b); a buck/boost switch ($Q_{b/b}$), a freewheeling diode (D_{fw}), an output capacitor (C*o*), etc.

The operating time period between buck and buck/boost converter depends on the boundary voltage, whose value is little more as compared to output voltage (*Vo*). The

DOI: http://dx.doi.org/10.17993/3ctecno.2019.specialissue3.201-219

converter operates in buck/boost mode as the input voltage (v_{in}) is lower than V_o and in buck mode for opposite condition (i-e $v_{in} > V_{boundary}$). Thus, the operating principle of the converter can be divided into two cases.

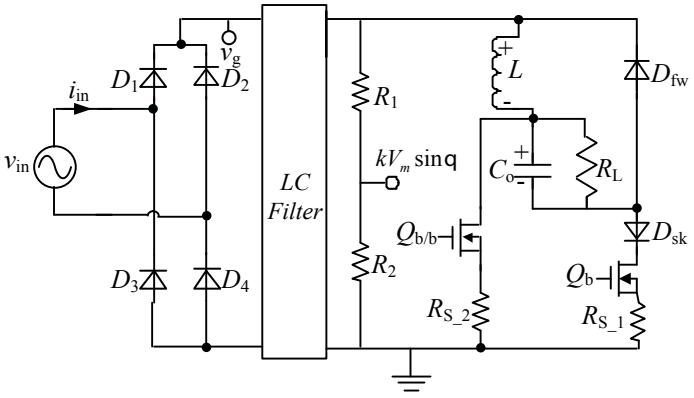

Figure 1. Schematic diagram of a CRM buck-buck/boost PFC converter.

The instantaneous and rectified input voltage during half line cycle can be given as:

$$v_{in} = v_a = V_m \sin\theta \tag{1}$$

Whereas V_m represent the input voltage amplitude, θ represent the input voltage angular frequency.

The converter is operating in buck mode when $v_{in} > V_{boundary}$. The buck/boost switch ($Q_{b/b}$) remain closed while buck switch (Q_b) keeps switching.

The maximum value of the inductor current and the average value of input current when the buck switch is conducting is respectively given as:

$$i_{L\_pk1} = \frac{V_m \sin\theta - V_o}{L} t_{on} \tag{2}$$

$$i_{in\_b} = \frac{V_o \left(V_m \sin\theta - V_o\right) t_{on}}{2LV_m \sin\theta} \tag{3}$$

The converter is operating in buck/boost mode when $v_{in} < V_{boundary}$. The buck/boost switch ($Q_{b/b}$) keeps switching, while buck switch (Q_b) remains closed.

Same as (2-3), the peak value of primary inductor and the average value of input current when $Q_{b/b}$ is switching is expressed respectively as:

$$i_{L\_pk_2} = \frac{t_{on} V_m \sin\theta}{L} \tag{4}$$

$$i_{in\_b/b} = \frac{V_o V_m \sin\theta}{2L\left(V_m \sin\theta + V_o\right)} t_{on} \tag{5}$$

By combining (3) and (5), the input current of the converter with traditional control is expressed as:

$$i_{in\_trad} = \begin{cases} \left(\dfrac{V_m \sin\theta}{V_m \sin\theta + V_o}\right)\dfrac{t_{on} V_o}{2L} & Q_b \; Conducting \\ \left(\dfrac{V_m \sin\theta - V_o}{V_m \sin\theta}\right)\dfrac{t_{on} V_o}{2L} & Q_{b/b} \; Conducting \end{cases} \tag{6}$$

The conducting angle of Q_b and $Q_{b/b}$ respectively given as:

$$\theta_0 \le \theta \le \pi - \theta_0 \tag{7}$$

$$0 \le \theta < \theta_0 \;\&\; \pi - \theta_0 < \theta \le \pi \tag{8}$$

Where θ_0 is the boundary angle between buck and buck/boost converter and is equal to arcsin $V_{boundary}/V_m$.

The average input power can be calculated from (1) and (6) as:

$$P_{in\_trad} = \frac{t_{on}}{2\pi L}\left[2\int_0^{\theta_0} \frac{V_o\left(V_m \sin\theta\right)^2}{\left(V_m \sin\theta + V_o\right)} d\theta + \int_{\theta_0}^{\pi-\theta_0} V_o\left(V_m \sin\theta - V_o\right) d\theta\right] \tag{9}$$

From (9), t_{on} can be determined by assuming the efficiency to be 100% as:

DOI: http://dx.doi.org/10.17993/3ctecno.2019.specialissue3.201-219

$$t_{on} = \frac{2\pi P_o L}{2\int_0^{\theta_0} \frac{V_o \left(V_m \sin\theta\right)^2}{\left(V_m \sin\theta + V_o\right)} d\theta + \int_{\theta_0}^{\pi-\theta_0} V_o \left(V_m \sin\theta - V_o\right) d\theta} \tag{10}$$

3. PROPOSED CONTROL SCHEME TO ATTAIN HIGH EFFICIENCY

For high efficiency and power balance, the input current must be:

$$i_{in\_VOTC} = \frac{2P_o \sin\theta}{V_m} \tag{11}$$

By combining (6) and (11), we can get required on-time of both switches as:

$$t_{on\_b} = u_{on} \frac{\left(V_m \sin\theta\right)^2}{V_o \left(V_m \sin\theta - V_o\right)} \tag{12(a)}$$

$$t_{on\_b/b} = u_{on} \left(\frac{V_m \sin\theta + V_o}{V_o} \right) \tag{12(b)}$$

The input power with put forward control scheme is given as:

$$P_{in\_prop} = \frac{1}{\pi} \int_0^{\pi} v_{in}\, i_{in}\, d\theta = \frac{u_{on} V_m^2}{4L} \tag{13}$$

The value of u_{on} is got as by assuming efficiency to be 100%

$$u_{on} = \frac{4P_o L}{V_m^2} \tag{14}$$

4. POWER LOSS ANALYSIS

The rms current of the on time period, i.e., the rms current of switch Q_b and $Q_{b/b}$ can be got as:

$$I_{rms(Q_{b/b}\_on)} = \frac{\sqrt{2\int_0^{\theta_0} i_{L(pk2)}^2(\theta)Dd\theta}}{3\pi} \quad (15(a))$$

$$I_{rms(Q_b\_on)} = \sqrt{\frac{\int_{\theta_0}^{\pi-\theta_0} i_{L(pk1)}^2(\theta)Dd\theta}{3\pi}} \quad (15(b))$$

The rms current of the off time period can be determined as:

$$I_{rms(Q_{b/b}\_off)} = \frac{\sqrt{2\int_0^{\theta_0} i_{L(pk2)}^2(\theta)[1-D]d\theta}}{3\pi} \quad (15(c))$$

$$I_{rms(Q_b\_off)} = \sqrt{\frac{\int_{\theta_0}^{\pi-\theta_0} i_{L(pk1)}^2(\theta)[1-D]d\theta}{3\pi}} \quad (15(d))$$

Where:

$$D = \begin{cases} \dfrac{V_o}{V_m \sin\theta} & Q_b\ Conducting \\ \dfrac{V_o}{V_o + V_m \sin\theta} & Q_{b/b}\ Conducting \end{cases} \quad (16)$$

While Q_b and $Q_{b/b}$ is on and off, the current flows through the winding of the inductor, whose rms current is:

$$I_{rms(trad)} = \sqrt{I_{rms(Q_b\_on\_trad)}^2 + I_{rms(Q_b\_off\_trad)}^2 + I_{rms(Q_{b/b}\_on\_trad)}^2 + I_{rms(Q_{b/b}\_off\_trad)}^2} \quad (17(a))$$

$$I_{rms(prop)} = \sqrt{I_{rms(Q_b\_on\_prop)}^2 + I_{rms(Q_b\_off\_prop)}^2 + I_{rms(Q_{b/b}\_on\_prop)}^2 + I_{rms(Q_{b/b}\_off\_prop)}^2} \quad (17(b))$$

4.1. BRIDGE RECTIFIER LOSS

Bridge rectifier loss can be calculated by using below formula:

$$P_{con\_bridge(trad)} = 2V_{FD}I_{in\_avg(trad)} \quad (18(a))$$

DOI: http://dx.doi.org/10.17993/3ctecno.2019.specialissue3.201-219

$$P_{con\_bridge(prop)} = 2V_{FD}I_{in\_avg(prop)} \tag{18(b)}$$

KBL10 is adopted as the rectifier bridge, whose forward voltage drop V_{FD} is 0.9 V. The input current with traditional and proposed control scheme is given as:

$$I_{in\_avg(trad)} = \frac{1}{\pi}\left[\begin{array}{l}\displaystyle\int_0^{\theta_0} \frac{\dfrac{\pi P_o V_o V_m \sin\theta}{(V_o + V_m \sin\theta)}}{\displaystyle\int_0^{\theta_0} \frac{V_o (V_m \sin\theta)^2}{(V_o + V_m \sin\theta)} d\theta + \int_{\theta_0}^{\pi/2} V_o (V_m \sin\theta - V_o) d\theta} d\theta \\ \displaystyle+\int_{\theta_0}^{\pi-\theta_0} \frac{\dfrac{V_o}{2}\left(\dfrac{V_m \sin\theta - V_o}{V_m \sin\theta}\right)}{\displaystyle\int_0^{\theta_0} \frac{V_o (V_m \sin\theta)^2}{(V_o + V_m \sin\theta)} d\theta + \int_{\theta_0}^{\pi/2} V_o (V_m \sin\theta - V_o) d\theta} d\theta\end{array}\right] \tag{19(a)}$$

$$I_{in\_avg(prop)} = \frac{4P_o}{\pi V_m} \tag{19(b)}$$

4.2. CONDUCTION LOSSES OF THE SWITCHES

The losses due to conduction of switches can be got as:

$$P_{con\_switches(trad)} = I^2_{rms(Q_b\_on\_trad)} R_{DS(on)\_Q_b} + I^2_{rms(Q_{b/b}\_on\_trad)} R_{DS(on)\_Q_{b/b}} \tag{20(a)}$$

$$P_{con\_switches(prop)} = I^2_{rms(Q_b\_on\_prop)} R_{DS(on)\_Q_b} + I^2_{rms(Q_{b/b}\_on\_prop)} R_{DS(on)\_Q_{b/b}} \tag{20(b)}$$

$R_{DS(On)}$ for the switch 20N60C3 is 0.19 Ω and the value is found from datasheet.

4.3. TURN OFF LOSSES OF THE SWITCHES

The turn off losses of buck and buck/boost switch with traditional and proposed control scheme can be determined as:

$$P_{off\_switches(trad)} = \frac{1}{\pi}\left[\begin{array}{l}\displaystyle 2\int_0^{\theta_0} \frac{i_{L(pk2,trad)}(V_m \sin\theta + V_o)}{2} t_{f1} f_{s(trad)} d\theta \\ \displaystyle+\int_{\theta_0}^{\pi-\theta_0} \frac{i_{L(pk1,trad)}(\theta) V_m \sin\theta}{2} t_{f2} f_{s(trad)} d\theta\end{array}\right] \tag{21(a)}$$

$$P_{off\_switches(prop)} = \frac{1}{\pi}\left[\begin{array}{l} 2\int_0^{\theta_0} \frac{i_{L(pk2,prop)}\left(V_m \sin\theta + V_o\right)}{2} t_{f1} f_{s(prop)} d\theta \\ +\int_{\theta_0}^{\pi-\theta_0} \frac{i_{L(pk1,prop)}(\theta) V_m \sin\theta}{2} t_{f2} f_{s(prop)} d\theta \end{array}\right] \quad (21(b))$$

The value of turn off fall time can be got from the datasheet which is 12ns for CMOS 20N60C.

The peak value of inductor current with both control scheme is given as:

$$i_{pk(trad)} = \begin{cases} i_{L(pk2,trad)} = \dfrac{\pi P_o V_m \sin\theta}{\int_0^{\theta_0} \dfrac{V_o\left(V_m \sin\theta\right)^2}{\left(V_o + V_m \sin\theta\right)} d\theta + \int_{\theta_0}^{\pi/2} V_o\left(V_m \sin\theta - V_o\right) d\theta} \\ i_{L(pk1,trad)} = \dfrac{\pi P_o\left(V_m \sin\theta - V_o\right)}{\int_0^{\theta_0} \dfrac{V_o\left(V_m \sin\theta\right)^2}{\left(V_o + V_m \sin\theta\right)} d\theta + \int_{\theta_0}^{\pi/2} V_o\left(V_m \sin\theta - V_o\right) d\theta} \end{cases} \quad (22(a))$$

$$i_{pk(prop)} = \begin{cases} i_{L(pk2,prop)} = \dfrac{4P_o \sin\theta\left(V_o + V_m \sin\theta\right)}{V_o V_m} \\ i_{L(pk1,prop)} = \dfrac{4P_o \sin^2\theta}{V_o} \end{cases} \quad (22(b))$$

The switching frequency in case of both control schemes can be found as:

$$i_{pk(trad)} = \begin{cases} i_{L(pk2,trad)} = \dfrac{\pi P_o V_m \sin\theta}{\int_0^{\theta_0} \dfrac{V_o\left(V_m \sin\theta\right)^2}{\left(V_o + V_m \sin\theta\right)} d\theta + \int_{\theta_0}^{\pi/2} V_o\left(V_m \sin\theta - V_o\right) d\theta} \\ i_{L(pk1,trad)} = \dfrac{\pi P_o\left(V_m \sin\theta - V_o\right)}{\int_0^{\theta_0} \dfrac{V_o\left(V_m \sin\theta\right)^2}{\left(V_o + V_m \sin\theta\right)} d\theta + \int_{\theta_0}^{\pi/2} V_o\left(V_m \sin\theta - V_o\right) d\theta} \end{cases} \quad (23(a))$$

$$i_{pk(prop)} = \begin{cases} i_{L(pk2,prop)} = \dfrac{4P_o \sin\theta\left(V_o + V_m \sin\theta\right)}{V_o V_m} \\ i_{L(pk1,prop)} = \dfrac{4P_o \sin^2\theta}{V_o} \end{cases} \quad (23(b))$$

DOI: http://dx.doi.org/10.17993/3ctecno.2019.specialissue3.201-219

The value of switching frequency is got as:

$$f_{s(trad)} = \begin{cases} \dfrac{V_o\left(\int_0^{\theta_0} \dfrac{V_o\left(V_m \sin\theta\right)^2}{V_o + V_m \sin\theta} d\theta + \int_{\theta_0}^{\pi/2} V_o\left(V_m \sin\theta - V_o\right) d\theta\right)}{\pi P_o L\left(V_o + V_m \sin\theta\right)} \\ \dfrac{V_o\left(\int_0^{\theta_0} \dfrac{V_o\left(V_m \sin\theta\right)^2}{V_o + V_m \sin\theta} d\theta + \int_{\theta_0}^{\pi/2} V_o\left(V_m \sin\theta - V_o\right) d\theta\right)}{\pi P_o L V_m \sin\theta} \end{cases} \quad (24(a))$$

$$f_{s(prop)} = \begin{cases} \dfrac{V_m^2 V_o}{2P_o L\left(V_o + V_m \sin\theta\right)^2} \\ \dfrac{V_o^2\left(V_m \sin\theta - V_o\right)}{4P_o L V_m \sin^3\theta} \end{cases} \quad (24(b))$$

4.4. COPPER LOSS OF THE INDUCTOR

The inductor's copper loss with traditional and proposed control scheme is given as:

$$P_{copper(prop)} = I_{rms(prop)}^2 R_{copper} \quad (25(a))$$

$$P_{copper(trad)} = I_{rms(trad)}^2 R_{copper} \quad (25(b))$$

The equivalent resistance of the copper wire is 0.156Ω.

4.5. CORE LOSS OF THE INDUCTOR

The inductor's core loss with traditional and proposed control scheme is calculated as:

$$P_{core(trad)} = \left[\int_0^{\pi} C_m f_{s(trad)}{}^x B_{ac(trad)}{}^y \left(ct_0 - ct_1 T_a - ct_2 T_a^2\right) d\theta\right] \frac{10^3 V_e}{\pi} \quad (26(a))$$

$$B_{ac(trad)} = \begin{cases} \dfrac{Li_{L(pk2,trad)}}{2NA_e} \\ \dfrac{Li_{L(pk1,trad)}}{2NA_e} \end{cases} \tag{26(b)}$$

$$P_{core(prop)} = \left[\int_0^{\pi} C_m f_{s(prop)}{}^{x} B_{ac(prop)}{}^{y} \left(ct_0 - ct_1 T_a - ct_2 T_a^2\right) d\theta\right] \frac{10^3 V_e}{\pi} \tag{26(c)}$$

$$B_{ac(prop)} = \begin{cases} \dfrac{Li_{L(pk2,prop)}}{2NA_e} \\ \dfrac{Li_{L(pk1,prop)}}{2NA_e} \end{cases} \tag{26(d)}$$

4.6. CONDUCTION LOSS OF THE FREEWHEELING DIODE

The conduction loss caused by freewheeling diode is given as:

$$P_{con\_freewheelingdiode(trad)} = \frac{V_{FD_{fw}}}{\pi} \int_0^{\pi} \frac{i_{pk(trad)}}{2} [1-D] d\theta \tag{27(a)}$$

$$P_{con\_freewheelingdiode(prop)} = \frac{V_{FD_{fw}}}{\pi} \int_0^{\pi} \frac{i_{pk(prop)}}{2} [1-D] d\theta \tag{27(b)}$$

The forward voltage drop for freewheeling diode MUR 1560 is 0.67.

4.7. THE THEORETICAL EFFICIENCY

The theoretical efficiency in case traditional and proposed control scheme can be calculated by using below formula:

$$\eta_{(trad)} = \frac{P_o}{\left[\begin{array}{l} P_o + P_{con\_bridge(trad)} + P_{con\_switches(trad)} + P_{off\_switches(trad)} \\ + P_{copper(trad)} + P_{core(trad)} + P_{con\_freewheelingdiode(trad)} \end{array}\right]} \tag{28(a)}$$

DOI: http://dx.doi.org/10.17993/3ctecno.2019.specialissue3.201-219

$$\eta_{(prop)} = \frac{P_o}{\left[\begin{array}{l} P_o + P_{con\_bridge(prop)} + P_{con\_switches(prop)} + P_{off\_switches(prop)} \\ + P_{copper(prop)} + P_{core(prop)} + P_{con\_freewheelingdiode(prop)} \end{array}\right]} \qquad (28(b))$$

Based on above analysis and parameter of the converter, loss distribution at 90VAC, 220VAC and theoretical efficiency is illustrated in Figure 2-4 respectively. It can be observed that by using proposed control scheme, the overall losses of the converter are reduced, and the efficiency is increased

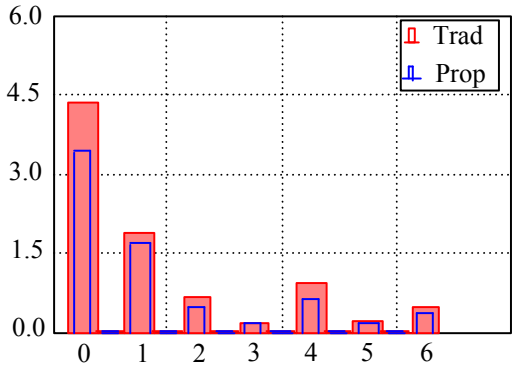

Figure 2. Loss distributions at 90VAC.

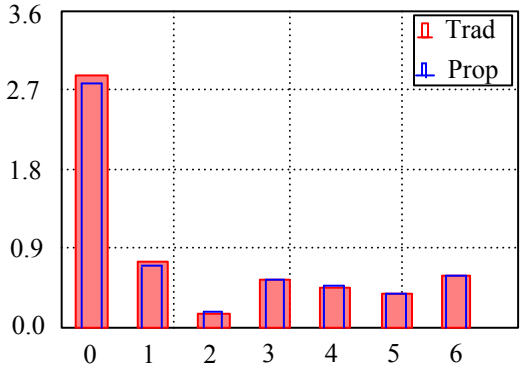

Figure 3. Loss distributions at 220VAC.

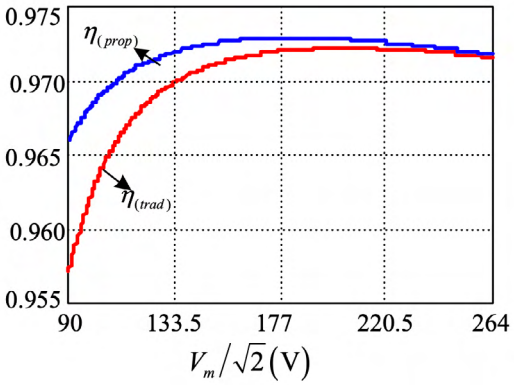

Figure 4. Efficiency at universal input voltage.

5. SIMULATION VERIFICATION

For verifying the effectiveness of proposed strategy, simulations are carried out. The input voltage range is 90-264VAC, and the output is 80V. For ensuring the current to be in CRM, L6561 IC is used. All the components in the circuit are selected as idea.

Figure 5 and Figure 6 show the simulation waveforms of v_{in} and i_{in} of the converter with traditional and proposed control scheme at 220VAC inputs, respectively. It can be observed that the input current with proposed control scheme is less in magnitude as compared to current with traditional control strategy. So the overall conduction losses will be less in case of VOTC as compared to COTC.

Figure 7 shows the switches' gate drive signals of the converter, from which in both types of control schemes, the converter operates either in buck mode or in buck/boost mode depending on the boundary voltage between them

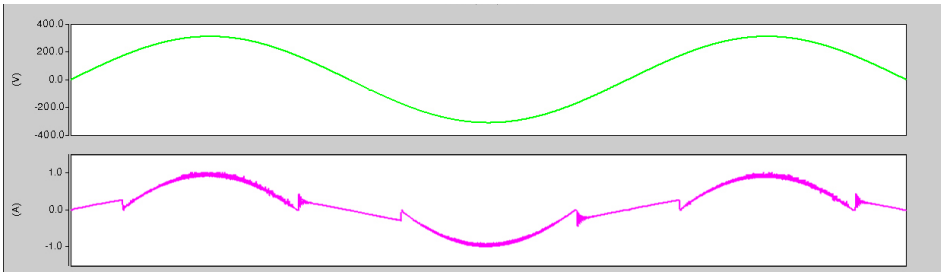

Figure 5. v_{in}& i_{in} with traditional control.

DOI: http://dx.doi.org/10.17993/3ctecno.2019.specialissue3.201-219

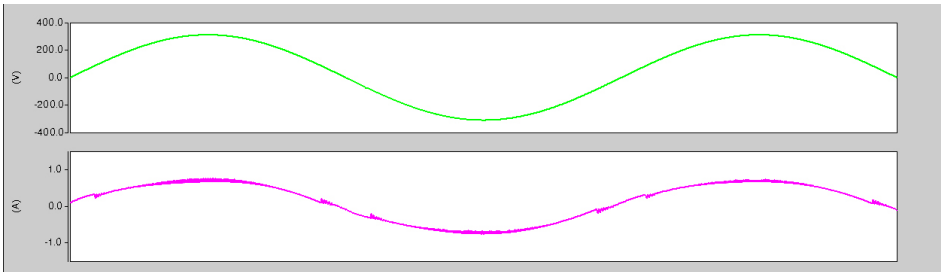

Figure 6. v_{in}&i_{in} with proposed control.

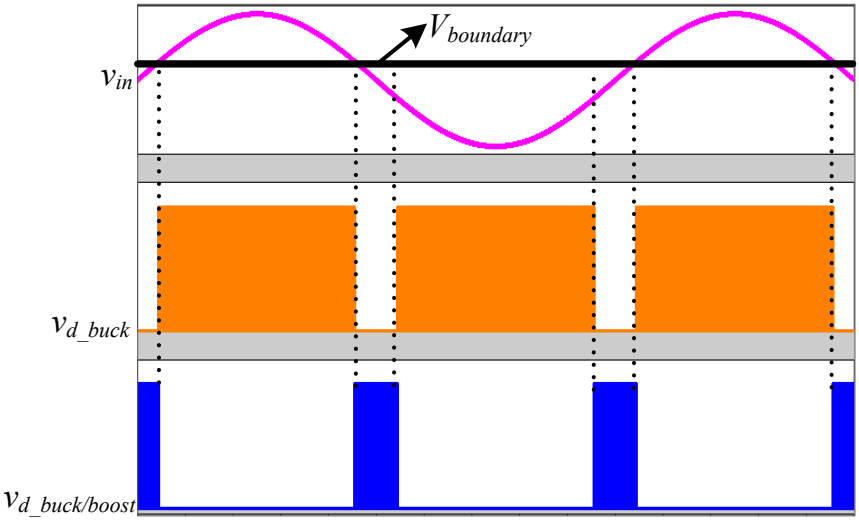

Figure 7. Switches' gate drive signals.

6. CONCLUSION

When the on-time is constant for buck-buck/boost converter, the conduction and switching losses are more because the rms and peak value of the inductor current is more. So, the efficiency is low. Thus, in this paper a control scheme is proposed to attain high efficiency with simple structure, minimum losses and minimum component cost. Simulation results are presented for the verification of the analysis.

REFERENCES

Alonso, J. M., Dalla Costa, M. A., & Ordiz, C. (2008). Integrated buck-flyback converter as a high-power-factor off-line power supply. *IEEE Transactions on Industrial Electronics, 55*(3), 1090-1100. doi: https://doi.org/10.1109/TIE.2007.908530

Dalla Costa, M. A., Alonso, J. M., Miranda, J. C., García, J., & Lamar, D. G. (2008). A single-stage high-power-factor electronic ballast based on integrated buck flyback converter to supply metal halide lamps. *IEEE Transactions on Industrial Electronics, 55*(3), 1112-1122. doi: https://doi.org/10.1109/TIE.2007.909729

Gacio, D., Alonso, J. M., Calleja, A. J., Garcia, J., & Rico-Secades, M. (2011). A universal-input single-stage high-power-factor power supply for HB-LEDs based on integrated buck-flyback converter. *IEEE Transactions on Industrial Electronics, 58*(2), 589-599. doi: https://doi.org/10.1109/TIE.2010.2046578

Gacio, D., Alonso, J. M., Garcia, J., Campa, L., Crespo, M. J., & Rico-Secades, M. (2012). PWM series dimming for slow-dynamics HPF LED drivers: The high-frequency approach. *IEEE Transactions on Industrial Electronics, 59*(4), 1717-1727. doi: https://doi.org/10.1109/TIE.2011.2130503

García, O., Cobos, J. A., Prieto, R., Alou, P., & Uceda, J. (2003). Single phase power factor correction: A survey. *IEEE Transactions on Power Electronics, 18*(3), 749-755. doi: https://doi.org/10.1109/TPEL.2003.810856

Langella, R., Testa, A., & Alii, E. (2014). IEEE recommended practice and requirements for harmonic control in electric power systems. In I*EEE Std 519-2014* (Revision of IEEE Std 519-1992), 1-29. doi: https://doi.org/10.1109/IEEESTD.2014.6826459

Memon, A. H., Yao, K., Chen, Q., Guo, J., & Hu, W. (2017). Variable-on-time control to achieve high input power factor for a CRM-integrated buck-flyback PFC converter. *IEEE Transactions on Power Electronics, 32*(7), 5312-5322. doi: https://doi.org/10.1109/TPEL.2016.2608839

Memon, A. H., & Yao, K. (2018). UPC strategy and implementation for buck-buck/boost PF correction converter. *IET Power Electronics, 11*(5), 884-894. doi: https://doi.org/10.1049/iet-pel.2016.0919

Memon, A. H., Baloach, M. H., Sahito, A. A., Soomro, A. M., & Memon, Z. A. (2018). Achieving High Input PF for CRM Buck-Buck/Boost PFC Converter. *IEEE Access*, 6, 79082-79093. doi: https://doi.org/10.1109/ACCESS.2018.2879804

Memon, A. H., Pathan, A. A., Kumar, M., Sahito, A. A J., & Memon, Z. A. (2019). Integrated buck-flyback converter with simple structure and unity power factor. *Indian Journal of Science and Technology, 12*(17). doi: https://doi.org/10.17485/ijst/2019/v12i17/144612

Memon, A. H., Memon, Z. A., Shaikh, N. N., Sahito, A. A., & Hashmani, A. A. (2019). Boundary conduction mode modified buck converter with low input current total harmonic distortion. *Indian Journal of Science and Technology, 12*(17). doi: https://doi.org/10.17485/ijst/2019/v12i17/144613

Memon, A. H., Shaikh, N. N., Kumar, M., & Memon, Z. A. (2019). Buck-buck/boost converter with high input power factor and non-floating output voltage. *International Journal of Computer Science and Network Security, 19*(4), 299-304. Retrieved from: http://paper.ijcsns.org/07_book/201904/20190442.pdf

Singh, B., Singh, S., Chandra, A., & Al-Haddad, K. (2011). Comprehensive study of single-phase AC-DC power factor corrected converters with high-frequency isolation. *IEEE transactions on Industrial Informatics, 7*(4), 540-556. doi: https://doi.org/10.1109/TII.2011.2166798

Spiazzi, G., & Buso, S. (2000). Power factor pre regulators based on combined buck-flyback topologies. *IEEE transactions on Power Electronics, 15*(2), 197-204. doi: https://doi.org/10.1109/63.838091

Xie, X., Zhao, C., Lu, Q., & Liu, S. (2013). A novel integrated buck-flyback nonisolated PFC converter with high power factor. *IEEE Transactions on Industrial Electronics, 60*(12), 5603-5612. doi: https://doi.org/10.1109/TIE.2012.2232256

Yao, K., Zhou, X., Yang, F., Yang, S., Cao, C., & Mao, C. (2017). Optimum third current harmonic during nondead zone and its control implementation to improve PF for DCM buck PFC converter. *IEEE Transactions on Power Electronics, 32*(12), 9238-9248. doi: https://doi.org/10.1109/TPEL.2017.2657883

Zhang, J., Zhao, C., Zhao, S., & Wu, X. (2017). A family of single-phase hybrid step-down PFC converters. *IEEE Transactions on Power Electronics, 32*(7), 5271-5281. doi: https://doi.org/10.1109/TPEL.2016.2604845

International Electrotechnical Commission. (2014). Part 3-2: Limits-Limits for harmonic current emissions (equipment input current≤16 A per phase). International Standard IEC, 61000-3-2.

Edición Especial Special Issue Noviembre 2019
DOI: http://dx.doi.org/10.17993/3ctecno.2019.specialissue3.201-219